# GC fingerprinting and immunomodulatory activity of polysaccharide from the rhizome of *Menispermum dauricum* DC

Pei Yang[1,#], Yang Zhai[2,#], Yan Ma[1], Beibei Mao[1], Fengshan Wang[3], Li Li[4], Lijuan Luan[2,*],
Yuhong Liu[1,*]

1 School of Pharmaceutical Sciences, Shandong University of Traditional Chinese Medicine,
Jinan 250355, China
2 Shandong Cancer Hospital and Institute, Shandong First Medical University and Shandong
Academy of Medical Sciences, Jinan 250117, China
3 NMPA Key Laboratory for Quality Research and Evaluation of Carbohydrate-based Medicine,
National Glycoengineering Research Center, School of Pharmaceutical Sciences, Shandong
University, Jinan 250012, China
4 Sishui Siheyuan Culture and Tourism Development Company, Ltd, Sisui 273200, China

*Corresponding author:
Yuhong Liu, yhliu@sdutcm.edu.cn
Lijuan Luan, 15553115573@163.com

#These authors have contributed equally to this work

## Abstract

This research aimed to establish the GC fingerprints and examine the immunomodulatory activity of the rhizome of *Menispermum dauricum* polysaccharides. In this study, the preparation conditions were optimized by the response surface method (RSM). Gas chromatography (GC) is an effective and sensitive technique employed to measure the composition of monosaccharides, the GC fingerprints of total polysaccharides from 10 batches of the rhizome of *M. dauricum* (tMDP) were established, and chemometrics methods were adopted to examine the differences and similarities of tMDP from distinct regions. The similarity evaluation illustrated that the polysaccharides derived from the rhizome of *M. dauricum* from different origins were highly similar. The results of principal components analysis (PCA) illustrated that all the tMDPs may be integrated into one group within the 95% confidence interval, but the rhizome of *M. dauricum* from different origins could also be distinguished in the plot of PCA scores. Then, the major

33    bioactive fraction MDP was purified and obtained by column chromatography. Our previous

34    study showed that MDP exhibited significant immunomodulatory activity, but the mechanism of

35    the in vitro immunomodulatory activity of MDP is unclear. The macrophage activation induced

36    by MDP was abolished when Toll-like receptor 4 (TLR4) signaling was knocked down by the

37    TLR4 inhibitor. Furthermore, western blot analysis illustrated that MDP activated RAW264.7

38    cells through MAPKs and NFκB pathways induced by TLR4. This research offers a theoretical

39    foundation for quality control and additional study as a potential immunomodulator of MDP.

40    **Keywords:** *Menispermum dauricum DC*; GC fingerprinting; immunomodulatory activity;

41    TLR4-MAPKs/NFκB

42    ## Introduction

43        The rhizome of *Menispermum dauricum DC* (Menispermaceae), referred to as Bei Dou Gen

44    in Chinese, which is mainly produced in northeastern, northern, and eastern China, is a

45    traditional Chinese medicine herb that has had widespread application in modern medicine to

46    treat diarrhea, sore throats, colitis, and rheumatic arthralgia, as well as other conditions (Wu, et

47    al., 2007). It contains various chemical components such as alkaloids, polysaccharides, quinones,

48    cardiac glycosides, lactones, saponins, tannins, proteins, and resins (Wu et al., 2018; Zhou et al.,

49    2018). The *M. dauricum* rhizome's main chemical components are alkaloids. These alkaloids

50    exert a variety of biological properties, including those that influence the cardiovascular system,

51    antitumor activity, and antiarrhythmic function. Additionally, the injection of total alkaloids has

52    been used therapeutically for a considerable period for the treatment of chronic tracheitis, as well

53    as arthralgia and throat sores (Chen et al., 2012).

54        The polysaccharides are also significant bioactive constituents of the rhizome of *M.*

55    *dauricum*, which exhibited numerous pharmacological properties while having no toxic effects

56    (Li, 2006; Liang, 2005; Lin, 2013a, b). In most cases, the quality control of polysaccharides is

57    primarily dependent on the phenol sulfuric acid technique, which involves establishing the

58    content of sugar present (Zhang et al., 2021). The phenol sulfuric acid approach, on the other

59    hand, is incapable of providing any structural properties of polysaccharides because of its low

60    level of specificity. Additionally, research suggested that adulterated or low-quality products

61    cannot be identified in an efficient manner(Li et al., 2019). Moreover, the biological properties of

62    polysaccharides are based on their numerous morphological characteristics, such as the

63    composition of their monosaccharides, the kind of glycosidic bonds, and the distribution of their

64    molecular weight (Li et al., 2019). In particular, the examination of the polysaccharide's

65    monosaccharide composition is the first and initial phase in the analysis of polysaccharides,

66    which needs to be taken into consideration to set up a quality control system for polysaccharides

67    and products associated with them.

68        Recently, the use of fingerprint profiling as a technology and methodology for quality

69    control of compounds generated from plants has gained widespread recognition as a practical

70    and effective technique (Li et al., 2019). In addition, chemometrics is a robust tool for analyzing

71    fingerprints premised on chemical data, such as principal component analysis (PCA) and

72    similarity analysis (SA), thus contributing to the analysis of the raw data gathered from

73    fingerprints (Dong et al., 2020; Liu et al., 2015a). Fingerprinting methods have been utilized

74    effectively to control quality as well as standardize plant polysaccharides, including *Panax,*

75    *Cordyceps*, *Ganoderma*, tea, and *Lycium barbarum* polysaccharides (Sun et al., 2014).

76        Polysaccharides derived from natural sources have garnered a lot of interest in recent years

77    because they do not have any toxic effects in studies to date and have potent immunomodulatory

78    properties (Pan et al., 2021; Zhong et al., 2021; Zhou et al., 2021). As a result, there is a

79    remarkable demand for the extraction and purification of new immunomodulatory

80    polysaccharides derived from natural products that are both safe and efficacious. Macrophages,

81    which are powerful phagocytic cells, are present in nearly all of the body's tissues. Macrophage

82    activation is an integral process in both adaptive and innate immune responses, which may

83    trigger and propagate defense responses against infections (Ma et al., 2019; Wang et al., 2017b).

84    Some botanical polysaccharides could be recognized and combined with specific receptors on

85    macrophages to enhance the viability of macrophages against pathogenic microorganisms and

86    tumorigenesis by the promotion of phagocytic and the cytokines of nitric oxide (NO), interleukin

87    (IL)-6 and tumor necrosis factor (TNF)-a (Yu et al., 2012). The polysaccharides with

88    immunomodulatory action that are derived from plant products have no reports of allergies or

89    adverse effects and have been believed to be potential candidates for use as immunoregulators

90    (Zhao et al., 2020).

91        In this research, the fingerprint of the rhizome *of M. dauricum* polysaccharide was

92    established and analyzed using GC and chemometrics, which offered a technique that was both

93    reliable and effective for controlling the quality of the rhizome *of M. dauricum* and provided the

94    groundwork for the future expansion of its functional products. Then, the major bioactive

95    fraction MDP was obtained by column chromatography. Moreover, the in vitro

96    immunomodulatory activities and the mechanism of MDP on macrophages were also evaluated.

97    **Materials and methods**

98    **Materials**

99        The rhizome of *M. dauricum* plants for each of the 10 batches, denoted by the letters S1 to

100   S10, was gathered from various regions throughout China (Table 1). The voucher samples of

101 rhizome of *M. dauricum* were deposited in the School of Pharmaceutical Sciences of Shandong

102 University of Traditional Chinese Medicine, Jinan, China.

103     Chemicals: The DEAE-cellulose-52 was procured from Yuanye Biological Co., Ltd.

104 (Shanghai, China). Sephadex G-50 and Sephacryl S-100 were procured from GE Healthcare Life

105 Sciences (Piscataway, NJ, USA). Guoyao Group Co., Ltd. (Beijing, China) provided glucose and

106 galactose. Arabinose, fucose, mannose, and rhamnose were all supplied by Macklin Biochemical

107 Technology Co., Ltd. (Shanghai, China). Lipopolysaccharide (LPS) was procured from Sigma-

108 Aldrich (St. Louis, MO, USA). The ELISA kits employed in the IL-6, NO, TNF-α, and IgM tests

109 were retrieved from Enzyme-linked Biotechnology Co., Ltd. (Shanghai, China). Antibodies

110 against MyD88, NFκB, JNK, ERK, and P38, as well as GAPDH, were procured from ABclonal

111 (Wuhan, China) while other antibodies were procured from Cell Signaling Technology (Beverly,

112 MA, USA).

113 **Experimental design of RSM**

114     The independent parameters chosen were the liquid-solid ratio (A, mL/g), extraction time

115 (B, min) and extraction temperature (C, ℃) whereas the dependent parameter was the

116 polysaccharide extraction yield, premised on the findings from the single-factor experiments.

117 The computation for the extraction yield was performed based on the formula below:

118     Extraction yield (%) = [crude polysaccharide weight (g)/ rhizome of *M. dauricum* weight

119 (g)] × 100%.

120     A three-factor three-level response surface optimization experiment and prediction model

121 were constructed with the aid of the Design-Expert software (version: 8.0.5).

122 **GC fingerprint analysis**

123 **Preparation of polysaccharide extracts**

124     Distilled water was used in the process of extracting crude polysaccharides from the

125 rhizome of *M. dauricum* under the optimal extraction parameters, which were determined

126 through response surface optimization. Following the completion of three rounds of extraction,

127 the aqueous extract was subjected to a vacuum and concentrated. After that, four times the

128 volume of ethanol was introduced into the solution to precipitate the polysaccharide, and

129 afterward, the mixture was left to stand at 4 °C for an entire night. The precipitate was collected

130 and deproteinized by means of the Trichloroacetic acid (TCA)-n-butanol method and then

131 subjected to freeze-drying to produce a total polysaccharide fraction (tMDP) (Yang et al., 2022).

132 **Complete acid hydrolysis**

133     Hydrolysis of 10 mg of tMDP was performed using 3 mL of 2 mol/L trifluoroacetic acid

134 (TFA) in a vial that was sealed at 110 ° C for six hours. To get rid of the TFA residue, the

135 mixture was combined with 1 mL of methanol, and then it was rotary-evaporated thrice under a

136 vacuum until it was completely dry. The hydrolyzed polysaccharide samples were prepared for

137 derivatization (Liu et al., 2015b).

138 **Preparation of Derivatization and GC analysis**

139   The GC method was employed to measure the composition of the monosaccharides. The

140 hydrolyzed tMDP and monosaccharide standards were added with hydroxylamine hydrochloride,

141 pyridine, and inositol hexaacetate, and stirred at 90 ℃ for 30 minutes. Then, acetic anhydride

142 was introduced and the reaction continued for 30min at 90℃ for acetylation. A GC examination

143 was performed on the products of the reaction. The temperature program was set to 170 ℃ for 3

144 minutes, 170 ℃ to 178 ℃ at a rate of 0.5 ℃/minutes for 3 minutes, and elevated to 210 ℃ for 5

145 minutes at a rate of 2 ℃/minutes (Yang et al., 2022).

146 **Extraction and purification of polysaccharides**

147   tMDP was extracted from the S10 batch (highest PCA score) of the rhizome of *M. dauricum*

148 by the method above, and the TCA-n-butanol method was used to remove protein. Subsequently,

149 the purification of tMDP was done utilizing the Sephadex G-50 column (1.75 cm×66 cm),

150 Sephacryl S-100 column (1.75 cm×66 cm), and DEAE-52 cellulose column (5.5 cm×30 cm), and

151 A white purified polysaccharide (MDP) was obtained by collecting the major fraction and

152 lyophilizing it (Yang et al., 2022).

153 **Immunomodulatory activity in vitro**

154 **Cell culture**

155   Beina Chuanglian Biotechnology Co., Ltd. (Beijing, China) provided the RAW264.7 cells

156 utilized in this study. At a temperature of 37 °C, the cells were incubated in DMEM that had

157 been supplemented with streptomycin sulfate (100 g/ml), penicillin (100 units/mL), and 10%

158 fetal bovine serum. The environment of the incubator was humidified and contained 5% carbon

159 dioxide.

160 **Cell viability test**

161   By conducting the Methyl thiazolyl tetrazolium (MTT) test in vitro, we examined the effect

162 that varying concentrations of MDP had on the RAW264.7 cells' viability. In general, 96-well

163 microplates were seeded with RAW264.7 cells at a density of $1×10^4$ cells per well. After the

164 cells had been cultured at 37 °C for 24 h with 5% carbon dioxide, they underwent a second round

165 of incubation at 37 °C for another 24 h with MDP samples at increasing dosages (0 µg/mL, 10

166 µg/mL, 50 µg/mL, 100 µg/mL, 200 µg/mL, and 400 µg/mL) or LPS (1 µg/mL, positive control).

167 Following the initial incubation, 20 µL of the MTT solution with a concentration of 5 mg/mL

168 was introduced into each well, and the plates were subsequently re-incubated at 37 °C for a

169 further 4 hours in the medium. After that, the medium was carefully aspirated, and each well was

170 then treated using 150 μL of DMSO so that the dissolving crystals could be dissolved. At last, to

171 ascertain the absorbance at 570 nm, we made use of a microplate reader (BioTek Instruments

172 Inc., Winooski, VT, USA) (Wang et al., 2017a).

173     Cell viability % = (OD treatment group)/(OD control group)×100%.

174 **TLR4 pathway blocking experiment**

175     RAW264.7 cells were seeded at a density of $1×10^4$ cells/well into 96-well microplates for

176 24 h. Following the adhesion of the cells, various doses of MDP (50, 100, and 200 μg/mL), as

177 well as LPS, were introduced, and TAK-242 was added at the same time to make the final

178 concentration of 20 μg/mL. Next, the concentrations of IL-6, TNF-α, and NO in the supernatant

179 were detected with the aid of ELISA kits (ML BIO Biotechnology, Shanghai, China) that are

180 commercially available. The assays were carried out in compliance with the guidelines that were

181 supplied by the manufacturer, after which the cytokine levels were calculated using the standard

182 curves.

183 **Western blotting analysis**

184     After cultivating the RAW 264.7 cells for 24 hours on a tissue culture plate with six wells

185 having a flat bottom at $5×10^6$ cells per well, the MDP was added at a final concentration of 50

186 μg/mL in order to activate these cells for twenty-four hours. The positive control consisted of the

187 cells that had been treated using LPS at a concentration of 1 μg/mL. At the end of the incubation

188 period, all of the conditioned cells were harvested and processed to produce the total proteins.

189 Briefly, samples were prepared by RIPA (radioimmune precipitation assay) with protease and

190 phosphatase inhibitors. The BCA technique was used to determine the protein. After

191 denaturation, 30 μg of protein per well was deposited via electrophoresis onto SDS-PAGE and

192 then transferred onto PVDF membranes. 10% nonfat milk (prepared in TBS supplemented with

193 0.1% Tween 20) was employed in blocking the membranes at ambient temperature for 4 h.

194 Afterward, the membranes were probed with primary antibodies against P38 (1:750), p-P38

195 (1:1000), ERK (1:1500), p-ERK (1:1500), JNK (1:1500), p-JNK (1:2000), NFκB (1:1500), p-

196 NFκB (1:1000), MyD88 (1:1500), TLR4 (1:1000), as per the guidelines stipulated by the

197 manufacturer. After being rinsed in TBST, the membranes were subjected to incubation with the

198 secondary antibody (1:5000) for one hour at ambient temperature. ECL chemiluminescence

199 detection kit (Millipore, Massachusetts, USA) was utilized to analyze the signals, which were

200 subsequently quantified with an Amersham Imager 600 Chemiluminescence imaging system

201 (GE, Boston, USA).

202 **Results**

**Extraction conditions optimization**

203
204     To maximize the extraction rate of polysaccharides and herb utilization, and to lay the
205     foundation for the subsequent fingerprinting study, RSM was adopted to generate optimal
206     conditions for extracting the rhizome of *M. dauricum* polysaccharides. Premised on the findings
207     obtained from the single-factor experimental analysis Fig. 1(a–c), a 3-factor 3-level response
208     surface experiment was carried out for optimizing the extraction conditions of polysaccharides.
209     To perform the variance analysis, we utilized the Design-Expert software (Table 2) to identify an
210     optimal region for the study by fitting the mathematical model with the experimental data.
211     To show the type of interaction between variables, 2D contour and 3D response surface
212     plots are presented in Fig. 1(d–i). According to the plots, the optimum extraction conditions for
213     polysaccharides were a ratio of liquid to the raw material of 19.79 mL/g, an extraction duration
214     of 116.47 min, and a temperature for extraction of 86.86 °C. The maximum anticipated
215     polysaccharides yield, under the optimal conditions, was 1.781%. However, for the sake of the
216     operability and convenience of production, there could be modifications to the experimental
217     parameters: the time for extraction was 116 min, the ratio of liquid to the raw material was 20
218     mL/g, and the temperature used for extraction was 87 °C.

219     **GC fingerprints analysis**
220     **GC fingerprints of tMDP**
221     tMDP was prepared by the optimized extraction conditions of RSM and deproteinization
222     using the TCA-n-butanol method, which was used to establish GC fingerprinting, thus laying the
223     foundation for controlling the quality of the rhizome of *M. dauricum*. To ascertain the structural
224     characteristics of polysaccharides, it is required and essential to take into account the
225     monosaccharide composition. Compositions of monosaccharides and polysaccharide ratios
226     varied remarkably by the source, which was an essential aspect of the polysaccharide's biological
227     activity. In the quality control of active polysaccharides throughout the last several years, the
228     monosaccharide composition-associated fingerprints have seen a widespread application. To
229     determine the standard GC fingerprint, GC was utilized to conduct monosaccharide composition
230     analysis on 10 different batches of tMDP. As shown in Fig.2A, GC fingerprinting of full acid
231     hydrolysates of 10 different batches of tMDP exhibited a high degree of similarity having 11
232     common peaks. Fig. 2B shows the fingerprint that was used as a reference. The chromatogram of
233     mixed standard monosaccharides depicted in Fig. 2C revealed the presence of seven different
234     components, with peaks 1, 2, 3, 8, 9, 10, and 11 representing rhamnose, arabinose, fucose,
235     mannose, glucose, galactose, and inositol (internal standard), respectively. To sum up the above,
236     tMDP contained six monosaccharides, among which rhamnose, glucose, and galactose were the

237     majority, whereas arabinose, fucose and mannose,    were of low content.

238     **The similarity analysis of the GC fingerprints**

239        Based on the professional program "Similarity Evaluation System for Chromatographic

240     Fingerprint of Traditional Chinese Medicine (TCM)" (Version 2012A), similarity values were

241     computed premised on the GC chromatograms of polysaccharide samples as well as the

242     reference fingerprint. Relative to the reference fingerprint, the similarity across 10 batches of

243     tMDP ranged from 0.943% to 0.998 (Table 3). The great similarity revealed that the previously

244     developed GC fingerprint was particularly suited as one of the multi-dimensional fingerprints for

245     quality control of the rhizomes of *M. dauricum*.

246     **PCA of the GC fingerprints**

247        The GC fingerprints of the rhizome of *M. dauricum* samples were then presented

248     quantitatively by utilizing PCA. The relative peak area of seven distinctive chromatographic

249     peaks (peaks 1, 2, 3, 4, 8, 9, and 10) in Fig. 2 was chosen in PCA. As depicted by the scree plot

250     (Fig. 3A), the first three PCs had eigenvalues of 4.302, 1.088, and 1.015, explaining 61.45%,

251     15.55%, and 14.50% of variance correspondingly, representing 91.50% of the total variance. The

252     following equations can be used to explain the principal components:

253     PC1=0.436*X1+0.437*X2+0.451*X3+0.255*X4+0.325*X8+0.387*X9+0.308*X10

254     PC2=-0.318*X1-0.156*X2-0.181*X3-0.735*X4+0.481*X8+0.061*X9-0.256*X10

255     PC3=0.114*X1-0.237*X2-0.180*X3-0.006*X4+0.362*X8-0.520*X9+0.704*X10

256        The PCA results were further analyzed by OriginPro 2021. As per the 3D scores plot of

257     PCA depicted in Fig. 3B, all of the rhizomes of *M. dauricum* samples were integrated into a

258     group within the 95% confidence ellipse, which indicated that the quality of the rhizome of *M.*

259     *dauricum* from Northeast and Shandong of China was similar, which was consistent with the

260     determination of polysaccharide content (Table 1). The high similarity suggested that the GC

261     fingerprint was very suitable as a quality control indicator for the rhizome of *M. dauricum*.

262     However, the rhizome of *M. dauricum* polysaccharides from different origins also differed

263     slightly and could be clustered into three categories broadly, among which S1, S2, S4, and S8

264     were all produced in Shandong, S3, S5, S7, and S10 were from Heilongjiang and Jilin, while S6

265     and S9 were from Liaoning.

266     **Immunomodulatory activity and mechanism of MDP**

267     **Effect of MDP on the morphology of RAW264.7 cells**

268        tMDP was further purified by cellulose and gel columns to obtain a homogeneous

269     polysaccharide fraction MDP. To examine the impact of MDP on RAW264.7 cells' morphology,

270     the morphologic changes of RAW264.7 cells were observed under a microscope. As could be

271    observed in Fig. 4A, the cells that belonged to the control group had a round shape and normal

272    structure. Nonetheless, following MDP treatment, there was a remarkable alteration in the

273    structure of the cells. It is quite clear to observe that many of the antennas generated surrounding

274    the cells may enhance the area of contact with exterior substances and were beneficial to the

275    phagocytic uptake. This suggests that concentrations of MDP ranging from 10 to 400 µg/mL are

276    capable of activating macrophages without causing cytotoxic effects.

277    **Effect of MDP on RAW264.7 cell viability**

278        Macrophages are the primary cells implicated in the innate defense mechanism of the

279    immune system. In addition, they are the major cells responsible for inflammation and other

280    immunological processes that occur inside the host. It has been shown that many different

281    polysaccharides stimulate both the activity of cells as well as their proliferation (Wang et al.,

282    2018). As a result, we studied how MDP affected the viability of RAW264.7 cells, and the

283    findings are depicted in Fig. 4B. At concentrations of 10, 50, 100, 200, and 400 µg/mL, the

284    levels of cell viability for the various groups were 120.66%, 123.64%, 118.76%, 130.02%, and

285    114.73%, correspondingly, which illustrate that MDP has the potential to significantly improve

286    RAW264.7 proliferation.

287    **MDP enhanced immunomodulatory effects via TLR4 in *vitro***

288        Macrophages are by far the most important body cells that are associated with the

289    immunological defense system (Cheng et al., 2019). After being activated, they are capable of

290    producing a wide variety of chemokines and cytokines. One of the most important mechanisms

291    that immunoregulators use is to cause the release of several biological components (IL-6, TNF-α,

292    NO, etc.) (Tian et al., 2019). NO is a type of vital molecule that is produced by macrophages,

293    and it played an important function in the modulation of apoptosis as well as the host's defense

294    against cancer cells and other pathogens (Ren et al., 2019). In addition, NO may also stimulate

295    phagocytosis and lysis in macrophages, two processes that are essential to the immune system.

296    Because of this, the ability of macrophages to release NO is an indication of the effects that

297    polysaccharides have on the functioning of the immune system (Wang et al., 2017a).

298    Inflammation, cancer, and immunological illnesses may all be traced back to the main active

299    molecules inside organisms, such as TNF-α and IL-6, which perform integral roles in the

300    pathogenesis of these conditions (Wang et al., 2017a). If the host is attacked by external

301    pathogens, activated macrophages produce IL-6 and TNF-α for the purpose of mediating the

302    immune system's response (Sorimachi et al., 1999). Our previous study showed that MDP could

303    promote the production of NO, IL-6 and TNF-α in RAW264.7 cells (Yang et al., 2022). These

304    results suggested that MDP has significant immunomodulatory activities via the mechanism of

305 increasing the release of NO, IL-6, and TNF-α in RAW264.7 cells. However, the mechanism of
306 the in vitro immunomodulatory activity of MDP is unclear.

307   TLRs have been discovered as key membrane receptors that perform an instrumental
308 function in activating macrophages (Fan et al., 2021). Among TLRs, several investigations have
309 demonstrated that TLR4 is implicated in the generation of cytokines in response to
310 polysaccharide stimulation (Liu et al., 2022b). To further investigate whether MDP exerts
311 immune activity through activation of the TLR4 pathway, TAK-242, an inhibitor of TLR4, was
312 utilized so that additional confirmation of the processes that result in MDP-mediated macrophage
313 activation could be achieved. As depicted in Fig. 5, TAK-242 considerably decreased the levels
314 of TNF-α, NO, and IL-6 ($P < 0.05$) as opposed to the MDP treatment group, illustrating that the
315 TLR4 pathway was implicated in the MDP-mediated activation of macrophages.

316 **MDP increased the protein expression of the TLR4-MAPK/NFκB signaling pathway**

317   By performing a Western blot analysis, we evaluated how MDP affected the protein
318 expression levels of TLR4 to get a deeper insight into its action mechanism. According to the
319 results shown in Fig. 6A, MDP significantly promoted the expression of TLR4 protein, which is
320 consistent with the above experimental results. Once TLR4 is activated, TLR4 is capable of
321 binding with the MyD88 protein to create the TLR4-MyD88 complex, which then stimulates the
322 phosphorylation of the downstream proteins, such as MAPKs (ERK, JNK, and p38) and NF-κB
323 (Xin et al., 2019). The findings of Western blotting (Fig. 6B) illustrated that the protein
324 expression of MyD88 was remarkably enhanced in RAW264.7 cells following MDP treatment,
325 which indicated that TLR4 protein, after being activated by MDP, combined with a large amount
326 of MyD88 and then activated the downstream pathway.

327   MAPKs perform crucial functions in immunological and inflammatory responses, including
328 the stimulation of cell proliferation and the regulation of cytokine production via the modulation
329 of transcriptional factors (Yang et al., 2019). Phosphorylation is a common mechanism that
330 underlies the functions that are controlled by MAPKs (Yang et al., 2019). To determine if the
331 MAPK signaling pathway was implicated in MDP-related macrophage activation, the
332 phosphorylation levels of the p38, ERK, and JNK MAPK pathways were examined through
333 western blot analysis. As depicted in Fig. 6D-F, the phosphorylation levels of ERK, JNK, and
334 p38 were substantially elevated in RAW264.7 cells following stimulation with MDP in contrast
335 with the normal control cells. It has been shown that NFκB is a ubiquitous transcriptional factor
336 that is essential for the activation of macrophages via the stimulation of diverse genes implicated
337 in the modulation of immunological as well as inflammatory responses (Yang et al., 2019). As
338 per the findings of Western blot (Fig. 6C), MDP caused an enhancement in the protein

339    expression of p-NFκB in RAW264.7 cells. In conclusion, following MDP treatment, the key

340    protein of TLR4-MAPK/NFκB signaling pathways including TLR4, MyD88, p- NFκB, p-ERK,

341    p-P38, and p-JNK were up-modulated substantially in RAW264.7 cells. As per these findings, it

342    is evident that MDP may stimulate the TLR4-MAPK/NFκB signaling pathways, which in turn

343    exerts immunomodulatory impacts.

**Discussion**

345      The detection methods commonly used for monosaccharide composition include high-

346    performance anion-exchange chromatography (HPAEC), gas chromatography (GC), and high-

347    performance liquid chromatography (HPLC) (Liu et al., 2022a). Among them, the GC is an

348    analytical method that is primarily utilized for characterizing and identifying volatile compounds

349    and is an effective and sensitive technique employed to measure the composition of

350    monosaccharides with the advantages of high sensitivity, good separation, fast analysis, and less

351    sample consumption (Liu et al., 2022a). Cheong et al. (Cheong et al., 2016) used GC and

352    HPSEC-RID-MALLS to compare and analyze the monosaccharide composition of three ginseng

353    plant polysaccharides, Ginseng, American ginseng, and Panax notoginseng, which all consisted

354    of six monosaccharides, but the intensity of each monosaccharide peak differed. This research

355    can both ensure the quality of certain polysaccharides found in *Panax* spp., and perform a

356    fundamental role in controlling the quality of the functional food products associated with these

357    polysaccharides. Ding et al. (Ding et al., 2020) established a fingerprint profile of *Lonicera*

358    *japonica* polysaccharide by GC, and the results of principal component analysis and factor

359    analysis showed that *L. japonica* produced in Shandong had the best quality and those produced

360    in Jilin were the last, indicating that different climatic environments could lead to differences in

361    quality of *L. japonica* herbs from different origins. It serves as a baseline for determining the

362    overall quality of herbs derived from *L. japonica*.

363      However, GC is not suitable for the determination of uronic acid fractions. Based on this,

364    we determined the monosaccharide composition of tMDP by thin-layer chromatography. The

365    results (Fig. S1) showed that tMDP did not contain uronic acid components, so GC could be used

366    to detect its monosaccharide composition. Additionally, GC fingerprints may be established to

367    offer a groundwork for the quality control of the rhizome of *M. dauricum* medicinal materials. A

368    total of 11 common peaks were obtained by GC fingerprinting of tMDP, and 6 peaks were

369    identified. Among them, peak 1 was Rha, peak 2 was Ara, peak 3 was Fuc, peak 8 was Man,

370    peak 9 was Glu, peak 10 was Gal, and peak 11 was internal standard. However, peaks 5, 7, and 8

371    were also present in the mixed standards, which may be by-products of the derivatization

372    process. Through GC fingerprinting and principal component analysis, the better quality herbs

373  were screened out, thus laying the foundation for subsequent experiments.

374  Polysaccharides have been demonstrated to perform a broad range of biological functions,

375  according to numerous studies, and the immunomodulatory activity of polysaccharides is widely

376  acknowledged to be the most significant biological function of these molecules. Macrophages

377  are immune cells that have a phagocytotic function to eliminate foreign antigens and perform an

378  instrumental function in the case of antimicrobial invasion and host defense (Liu et al., 2022b).

379  By coming into close touch with or eliminating infections or tumor cells, activated macrophages

380  may generate cytokines that trigger other immune cells (Liu et al., 2022b). In this study, MDP

381  was found to activate RAW264.7 cells and enhance the secretion of TNF-α, NO, and IL-6

382  indicating that MDP has immunomodulatory properties. Furthermore, the influence of MDP in

383  promoting the release of TNF-α, NO, and IL-6 was suppressed after TAK-242 treatment. This

384  suggests the possibility that MDP exerts immunomodulatory activity by activating the TLR4

385  protein pathway. The connection between the MAPK, TLR4, and TLR4 signaling pathways is

386  known. When TLR4 is expressed in RAW264.7 cells, it activates two distinct signaling

387  networks: the TRIF-dependent pathways and the MyD88-dependent pathways. Once the TLR4

388  signaling pathway has been activated, it stimulates the activation of the NF-κB and MAPK

389  signaling pathways in a mechanism that is reliant on MyD88. The findings of western blotting

390  illustrated that MDP could activate the expression of key node proteins on the TLR4-

391  MAPK/NFκB pathway. In summary, the results of our research showed that MDP does, in fact,

392  remarkably activate macrophages by activating TLR4, which is mediated by MAPK and NFκB

393  signaling pathways (Fig. 7). This signaling pathway has also been shown to be responsible for

394  the immunomodulatory activities of other polysaccharides, according to multiple research reports

395  (Yang et al., 2019; Liu et al., 2022a; Wu et al., 2019).

396  **Conclusions**

397  In this research, the extraction conditions of polysaccharides from the rhizome of *M.

398  dauricum* were successfully optimized by RSM. The GC fingerprints of 10 batches of the

399  rhizome of *M. dauricum* polysaccharides were established, and The findings of SA and PCA of

400  the fingerprints illustrated that the rhizome of *M. dauricum* polysaccharides derived from various

401  sources each had their own distinct chromatographic fingerprint features. Moreover, according to

402  the findings of this research, MDP may substantially activate RAW264.7 cells through the

403  TLR4-MAPK/NFκB dependent signaling pathway so as to generate biological cytokines. In

404  conclusion, our studies have demonstrated an in vitro immunomodulatory effect of MDP with a

405  molecular mechanism that is related to the activation of the TLR4-MAPK/NFκB signaling

406  pathway.

## Abbreviations

GC, Gas chromatography; RSM, Response surface method; tMDP, Total polysaccharides from the rhizome of *M. dauricum*; MDP, Polysaccharides from the rhizome of *M. dauricum*; PCA, Principal components analysis; TLR4, Toll-like receptor 4; MyD88, Myeloid differentiation factor 88 protein; MAPK, Mitogen-activated protein kinase; NFκB, Nuclear factor kappa-B; TCA, Trichloroacetic acid; TFA, Trifluoroacetic acid; MTT, Methyl thiazolyl tetrazolium; LPS, Lipopolysaccharide; RIPA, Radioimmune precipitation assay; BCA, Bicinchoninic acid.

## Funding

We received support in the form of grants from the National Natural Science Foundation of China (81973218), Taishan Industry Leading Talents Project (tscy20200410), Technology Development Program of TCM of Shandong Province (2019-0024), Open Projects Fund of NMPA Key Laboratory for Quality Research and Evaluation of Carbohydrate-based Medicine (No. 2021QRECM02) and Shandong Key Laboratory of Carbohydrate Chemistry and Glycobiology, Shandong University (2021CCG05).

## References

Chen, J. Y., Xie, Y. F., Zhou, T. X., Qin, G. W., 2012. Chemical constituents of Menispermum dauricum:Chemical constituents of Menispermum dauricum. Chin. J. Nat. Med. 10(4).

Cheng, X. D., Wu, Q. X., Zhao, J., Su, T., Lu, Y. M., & Zhang, W. N., et al., 2019. Immunomodulatory effect of a polysaccharide fraction on RAW 264.7 macrophages extracted from the wild lactarius deliciosus. Int. J. Biol. Macromol. 128, 732-739.

Cheong, K. L., Wu, D. T., Deng, Y., Leong, F., Zhao, J., Zhang, W. J., Li, S. P., 2016. Qualitation and quantification of specific polysaccharides from Panax species using GC-MS, saccharide mapping and HPSEC-RID-MALLS. Carbohydr. Polym. 153, 47-54.

Ding, J., 2020. Study on Fingerprint and in vitro Antiviral Activity of Lonicera japonica Polysaccharide. Chin. Pharmacy. 31, 1061-1067.

Dong, Y., Pei, F., Su, A., Sanidad, K. Z., Ma, G., Zhao, L., Hu, Q., 2020. Multiple fingerprint and fingerprint-activity relationship for quality assessment of polysaccharides from Flammulina velutipes. Food. Chem. Toxical. 135, 110944.

Fan, S., Wang, Y., Zhang, Y., Wu, Y., & Chen, X., 2021. *Achyranthes bidentata* Polysaccharide Activates Nuclear Factor-Kappa B and Promotes Cytokine Production in J774A.1 Cells Through TLR4/MyD88 Signaling Pathway. Front. Pharmacol. *12*, 753599.

Li, H., Gong, X., Wang, Z., Pan, C., Zhao, Y., Gao, X., Liu, W., 2019. Multiple fingerprint profiles and chemometrics analysis of polysaccharides from Sarcandra glabra. Int. J. Biol. Macromol. 123, 957-967.

Li, M., Shan, B. E., Liang, W. J., Ren, F. Z., 2006. Experimental study on the antimutagenic and mutagenic activity of Rhizoma menispermi extracts. Chin. J. Cancer. Prev. Treat. 411-413.

Liang, W. J., Liu, D. Q., Shan, B. E., Zhang, J., Li, Q. X., 2005. Study of immunoregulatory activity of rhizoma menipermi extracts on mouse and human lymphocytes and macrophages in vitro. Chin. J. Immunology. 56-59.

Lin, M., Xia, B.R., Yang, M., Gao, S., Huo, Y.Q., Lou, G., 2013a. Anti-ovarian cancer potential of two acidic polysaccharides from the rhizoma of Menispermum dauricum. Carbohydr. Polym. 92.

Lin, M., Xia, B.R., Yang, M., Gao, S., Huo, Y.Q., Lou, G., 2013b. Characterization and antitumor activities of a polysaccharide from the rhizoma of Menispermum dauricum. Int. J. Biol. Macromol. 53.

Liu, J., 2022a. Research Progress on Fingerprint Analysis and Profile-EffectRelationship of Polysaccharides. Sci. Tech. Food. Ind. 43, 404-412.

456   Liu, W., Xu, J., Zhu, R., Zhu, Y., Zhao, Y., Chen, P., Pan, C., Yao, W., Gao, X., 2015a.
457        Fingerprinting profile of polysaccharides from Lycium barbarum using multiplex
458        approaches and chemometrics. Int. J. Biol. Macromol. 78, 230-237.
459   Liu, X., Chen, X., Xie, L., Xie, J., Shen, M., 2022b. Sulfated Chinese yam polysaccharide
460        enhances the immunomodulatory activity of RAW 264.7 cells via the TLR4-MAPK/NF-κB
461        signaling pathway. Food & Funct.
462   Liu, Y. H., Liu, C. H., Jiang, H. Q.,   Zhou, H. L.,   Li, P. L., & Wang, F. S., 2015b. Isolation,
463        structural characterization and neurotrophic activity of a polysaccharide from phellinus
464        ribis. Carbohydr. Polym.
465   Ma, L., Jiao, K., Luo, L., Xiang, J., Fan, J., Zhang, X., Yi, J., Zhu, W., 2019. Characterization
466        and macrophage immunomodulatory activity of two polysaccharides    from the flowers of
467        Paeonia suffruticosa Andr. Int. J. Biol. Macromol. 124, 955-962.
468   Pan, Q., Sun, Y., Li, X., Zeng, B., Chen, D., 2021. Extraction, structural characterization, and
469        antioxidant and immunomodulatory activities of a polysaccharide from Notarchus leachii
470        freeri eggs. Bioorg. Chem. 116, 105275.
471   Ren, D., Zhao, Y., Zheng, Q., Alim, A., & Yang, X., 2019. Immunomodulatory effects of an
472        acidic polysaccharide fraction from herbal gynostemma pentaphyllum tea in RAW264.7
473        cells. Food & Funct.
474   Sorimachi, K., Akimoto, K., Hattori, Y., Ieiri, T., & Niwa, A., 1999. Secretion of TNF-α, IL-8
475        and nitric oxide by macrophages activated with polyanions, and involvement of interferon-γ
476        in the regulation of cytokine secretion. Cytokine, 11(8), 571-578.
477   Sun, X., Wang, H., Han, X., Chen, S., Zhu, S., Dai, J., 2014. Fingerprint analysis of
478        polysaccharides from different Ganoderma by HPLC combined with chemometrics
479        methods. Carbohydr. Polym. 114, 432-439.
480   Tian, H., Liu, Z. J., Pu, Y. W.,Bao Y. X., 2019. Immunomodulatory effects exerted by poria
481        cocos polysaccharides via TLR4/TRAE6/NF-κB signaling in vitro and in vivo. Biomed.
482        Pharmacother.
483   Wang, M., Yang, X. B., Zhao, J. W., Lu, C. J., & Zhu, W., 2017a. Structural characterization and
484        macrophage immunomodulatory activity of a novel polysaccharide from smilax glabra
485        roxb. Carbohydr. Polym.,156, 390-402.
486   Wang, Y., Tian, Y., Shao, J., Shu, X., Jia, J., Ren, X., Guan, Y., 2018. Macrophage
487        immunomodulatory activity of the polysaccharide isolated from Collybia radicata
488        mushroom. Int. J. Biol. Macromol. 108, 300-306.

489    Wang, Z., Liu, Z., Zhou, L., Long, T., Zhou, X., Bao, Y., 2017b. Immunomodulatory effect of
490        APS and PSP is mediated by Ca2(+)-cAMP and TLR4/NF-kappaB signaling pathway in
491        macrophage. Int. J. Biol. Macromol. 94, 283-289.
492    Wu, D., Du, J.K., Zhang, Y., Su, Y., Zhang, H., 2018. Anti-tumor effects of phenolic alkaloids of
493        menispermum dauricum on gastric cancer in vivo and in vitro . J. Cancer. Res. Ther. 14.
494    Wu M. X., Jin L. Q., 2007. The Research Progress of the rhizoma of Menispermum dauricum.
495        Mod. Chin. Med. 09, 35-38.
496    Wu, Y.G., Wang, K.W., Zhao, Z.R., Zhang, P., Liu, H., & Zhou, G.J., et al., 2019. A novel
497        polysaccharide from Dendrobium devonianum serves as a TLR4 agonist for activating
498        macrophages. Int. J. Biol. Macromol. 133.
499    Xin, X., Ma, L.M., Zhou, Y.R., Shen, W., Xu, D.Y., Dou, J., et al., 2019. Polysaccharide
500        enhanced NK cell cytotoxicity against pancreatic cancer via TLR4/MAPKs/NF-κB pathway
501        in vitro/vivo. Carbohydr. Polym. 225.
502    Yang, F., Li,X.Z., Yang, Y., Ayivi-Tosuh, S.M., Wang, F., Li, H., 2019. A polysaccharide
503        isolated from the fruits of Physalis alkekengi L. induces RAW264.7 macrophages activation
504        via TLR2 and TLR4-mediated MAPK and NF-κB signaling pathways. Int. J. Biol.
505        Macromol. 140.
506    Yang, P., Jin, J., Ma, Y., Wang, F.S., Li, Y.Y., Duan, B.G., et al., 2022. Structure
507        Characterization, Immunological Activity, and Mechanism of a Polysaccharide From the
508        Rhizome of *Menispermum dauricum* DC. Front. Nutr.
509    Yu, Q., Nie, S. P., Wang, J. Q., Yin, P. F., Li, W. J., Xie, M. Y., 2012. Polysaccharide from
510        Ganoderma atrum induces tumor necrosis factor-alpha secretion via phosphoinositide 3-
511        kinase/Akt, mitogen-activated protein kinase and nuclear factor-kappaB signaling pathways
512        in RAW264.7 cells. Int. Immunopharmacol. 14, 362-368.
513    Zhang, Y., Wu, M., Xi, J., Pan, C., Xu, Z., Xia, W., Zhang, W., 2021. Multiple-fingerprint
514        analysis of Poria cocos polysaccharide by HPLC combined with chemometrics methods. J.
515        Pharm. Biomed. Anal. 198, 114012.
516    Zhao Y.,Yan B. C., Wang Z. Y., Li M. J., Zhao W., 2020. Natural Polysaccharides with
517        Immunomodulatory Activities. Mini Rev Med Chem. 20(2).
518    Zhong, R. F., Yang, J. J., Geng, J. H., Chen, J., 2021. Structural characteristics, anti-proliferative
519        and immunomodulatory activities of a purified polysaccharide from Lactarius volemus Fr.
520        Int. J. Biol. Macromol. 192, 967-977.

521 Zhou, Y. L., Zhao, X., Li, S. X., Lv, H. M., Wang, A. L., Zhang, Y., 2018. Alkaloids from

522   Rhizome of Menispermum dauricum and Their Anti-inflammatory Activity. Mod. Chin.

523   Med. 20, 163-168.

524 Zhou, Y., Wang, S., Feng, W., Zhang, Z., Li, H., 2021. Structural characterization and

525   immunomodulatory activities of two polysaccharides from Rehmanniae Radix Praeparata.

526   Int. J. Biol. Macromol. 186, 385-395.

The source, neutral sugar content and principal component analysis composite score of the total polysaccharides from the rhizome of *M. dauricum*

1     Table 1 The source, neutral sugar content and principal component analysis composite score

2                of the total polysaccharides from the rhizome of *M. dauricum*

| NO. | Source | Neutral sugar content (%) | Principal component analysis composite score |
|-----|--------|---------------------------|---------------------------------------------|
| S1 | Shandong | 20.34 | -1.777427 |
| S2 | Shandong | 19.54 | 0.0950919 |
| S3 | Heilongjiang | 20.32 | 0.8092878 |
| S4 | Shandong | 20.77 | -1.506477 |
| S5 | Heilongjiang | 19.47 | -0.156665 |
| S6 | Liaoning | 22.77 | 0.6893036 |
| S7 | Jilin | 20.12 | 0.5907167 |
| S8 | Shandong | 21.91 | 0.1607214 |
| S9 | Liaoning | 22.61 | -1.386776 |
| S10 | Jilin | 20.86 | 2.4822341 |

Analysis of variance in the regression model

Note: **$P<0.01$ significant different.

1             Table 2 Analysis of variance in regression model

| Source | Square sum | df | Mean square | F value | P value | Significance |
|---|---|---|---|---|---|---|
| Model | 0.69 | 9 | 0.077 | 357.11 | <0.0001 | ** |
| A-A | 0.0072 | 1 | 0.0072 | 33.60 | 0.0007 | ** |
| B-B | 0.00845 | 1 | 0.00845 | 39.43 | 0.0004 | ** |
| C-C | 0.029 | 1 | 0.029 | 134.4 | <0.0001 | ** |
| AB | 0.000225 | 1 | 0.000225 | 1.05 | 0.3396 | |
| AC | 0.000625 | 1 | 0.000625 | 2.92 | 0.1314 | |
| BC | 0.000225 | 1 | 0.000225 | 1.05 | 0.3396 | |
| $A^2$ | 0.43 | 1 | 0.43 | 1996.38 | <0.0001 | ** |
| $B^2$ | 0.13 | 1 | 0.13 | 593.19 | <0.0001 | ** |
| $C^2$ | 0.037 | 1 | 0.037 | 172.7 | <0.0001 | ** |
| Residual | 0.00150 | 7 | 0.0002143 | | | |
| Lack of Fit | 0.0009 | 3 | 0.0003 | 2.0 | 0.2564 | |
| Pure Error | 0.0006 | 4 | 0.00015 | | | |
| Cor Total | 0.69 | 16 | | | | |

2    Note: **$P<0.01$ significant different.

Similarity analysis of 10 batches of tMDP

Table 3 Similarity analysis of 10 batches of tMDP

| NO. | S1 | S2 | S3 | S4 | S5 | S6 | S7 | S8 | S9 | S10 | R |
|---|---|---|---|---|---|---|---|---|---|---|---|
| S1 | 1.000 | 0.984 | 0.990 | 0.997 | 0.990 | 0.990 | 0.989 | 0.973 | 0.977 | 0.988 | 0.995 |
| S2 | 0.984 | 1.000 | 0.977 | 0.988 | 0.977 | 0.976 | 0.975 | 0.998 | 0.964 | 0.958 | 0.987 |
| S3 | 0.990 | 0.977 | 1.000 | 0.991 | 0.998 | 0.993 | 0.998 | 0.968 | 0.996 | 0.994 | 0.998 |
| S4 | 0.997 | 0.988 | 0.991 | 1.000 | 0.990 | 0.995 | 0.990 | 0.977 | 0.981 | 0.987 | 0.997 |
| S5 | 0.990 | 0.977 | 0.998 | 0.990 | 1.000 | 0.990 | 0.998 | 0.970 | 0.993 | 0.991 | 0.997 |
| S6 | 0.990 | 0.976 | 0.993 | 0.995 | 0.990 | 1.000 | 0.992 | 0.963 | 0.988 | 0.993 | 0.996 |
| S7 | 0.989 | 0.975 | 0.998 | 0.990 | 0.998 | 0.992 | 1.000 | 0.967 | 0.997 | 0.994 | 0.997 |
| S8 | 0.973 | 0.998 | 0.968 | 0.977 | 0.970 | 0.963 | 0.967 | 1.000 | 0.955 | 0.943 | 0.979 |
| S9 | 0.977 | 0.964 | 0.996 | 0.981 | 0.993 | 0.988 | 0.997 | 0.955 | 1.000 | 0.990 | 0.992 |
| S10 | 0.988 | 0.958 | 0.994 | 0.987 | 0.991 | 0.993 | 0.994 | 0.943 | 0.990 | 1.000 | 0.991 |
| R | 0.995 | 0.987 | 0.998 | 0.997 | 0.997 | 0.996 | 0.997 | 0.979 | 0.992 | 0.991 | 1.000 |

# Figure 1

Influences of extraction variables on the polysaccharides yield from the rhizome of *M. dauricum* ; response surface plots and contour plots.

(a) Effect exerted by the liquid/solid ratio (mL/g) on polysaccharides yield from the rhizome of *M. dauricum*; (b) Effect exerted by the extraction time (min) on polysaccharides yield from the rhizome of *M. dauricum*; (c) Effect exerted by the extraction temperature (°C) on polysaccharides yield from the rhizome of *M. dauricum*; (d) plots of response surface presenting the interactive effects of liquid/solid ratio (A) and extraction time (B); (e) response surface plots presenting the interactive effects of liquid/solid ratio (A) and extraction temperature (C); (f) response surface plots presenting the interactive effects of extraction duration (B) and extraction temperature (C); (g) contour plots presenting the interactive effects of A and B; (h) contour plots presenting the effects of the interaction of A and C; (i) contour plots presenting the interactive effects of B and C. The values are presented as the mean ± SD, n = 3.
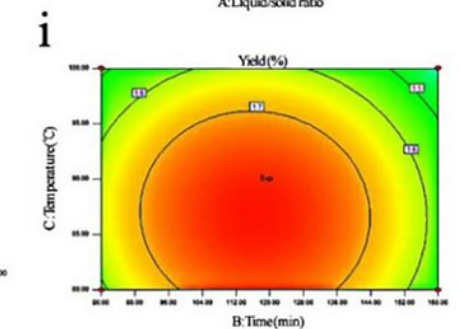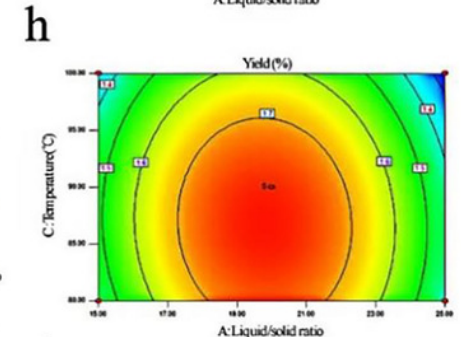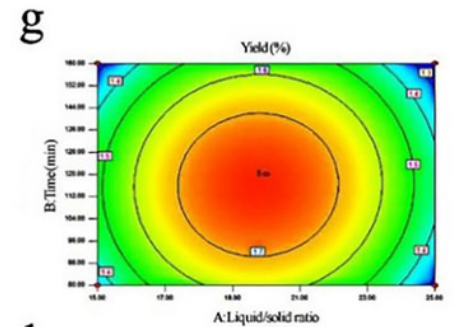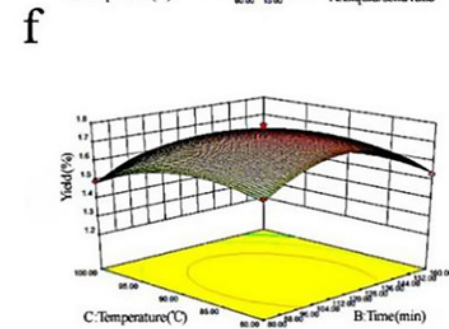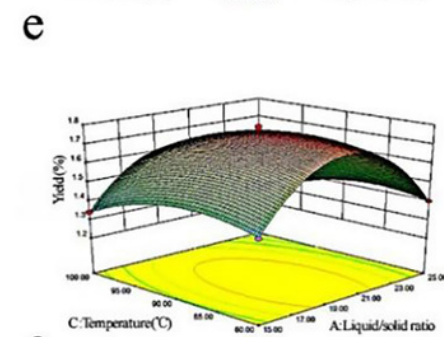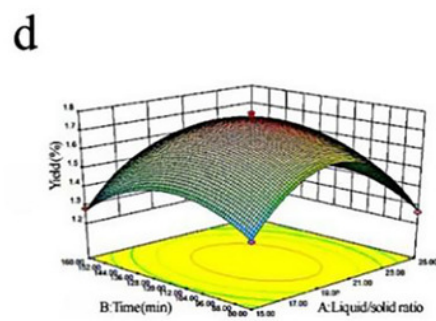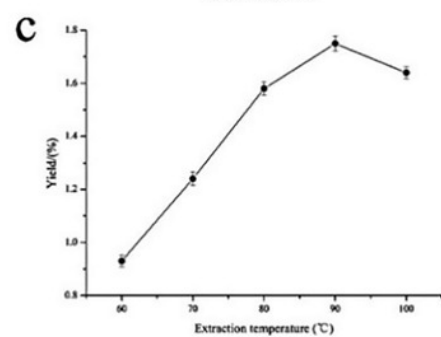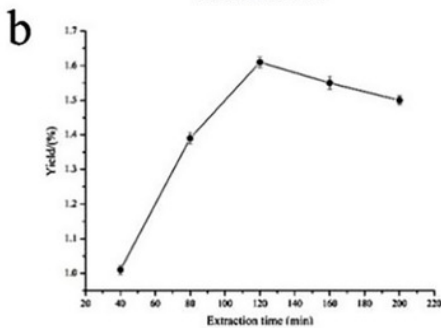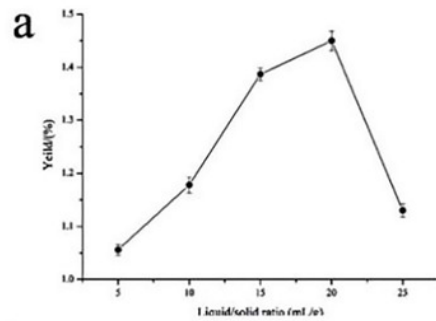
# Figure 2

GC chromatograms of 10 different batches of tMDP's complete acid hydrolysates (A), the reference GC fingerprint of tMDP (B), Monosaccharide standards, and tMDP sample (1, Rhamnose ; 2, Arabinose; 3, Fucose; 8, Mannose; 9, Glucose ; 10, Galactose ; 11,
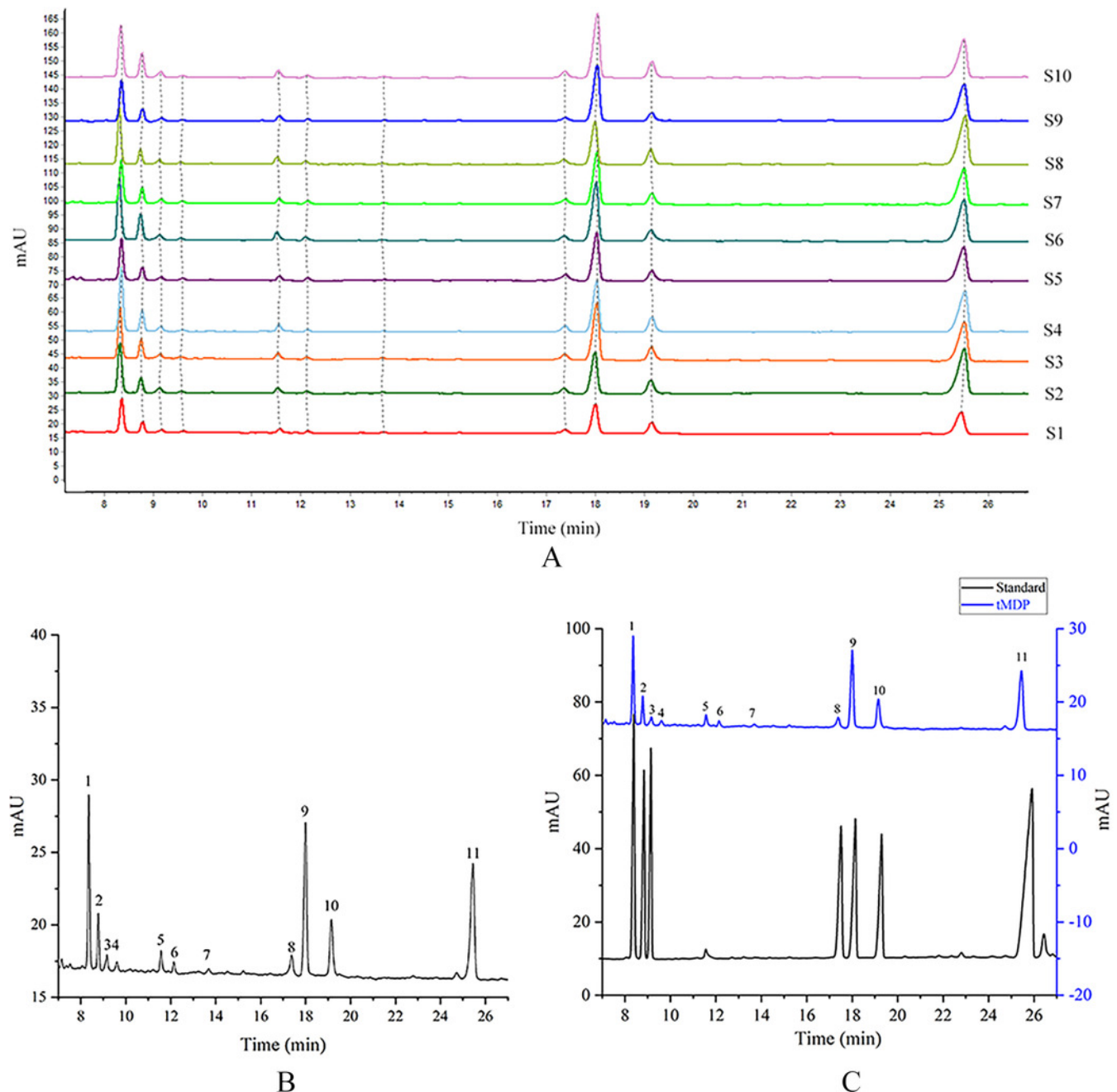
# Figure 3

The scree plot (A) and plot of PCA scores (B) of tMDP' GC fingerprints from different regions.
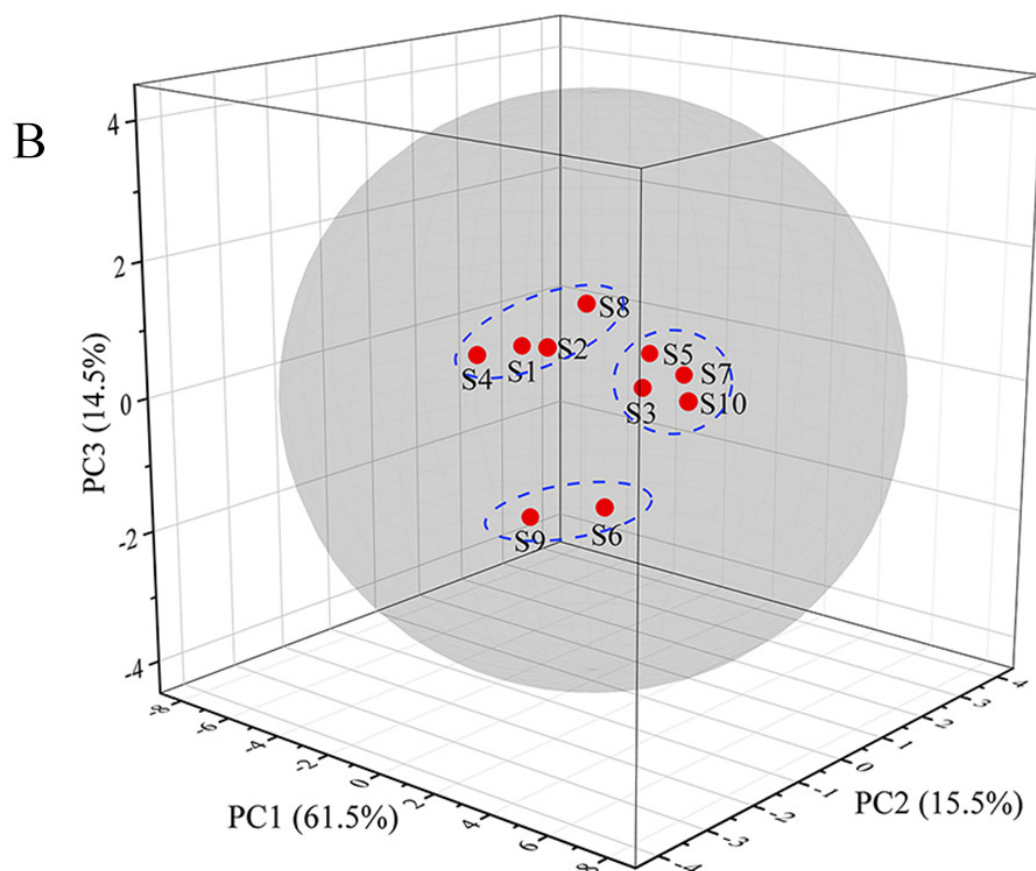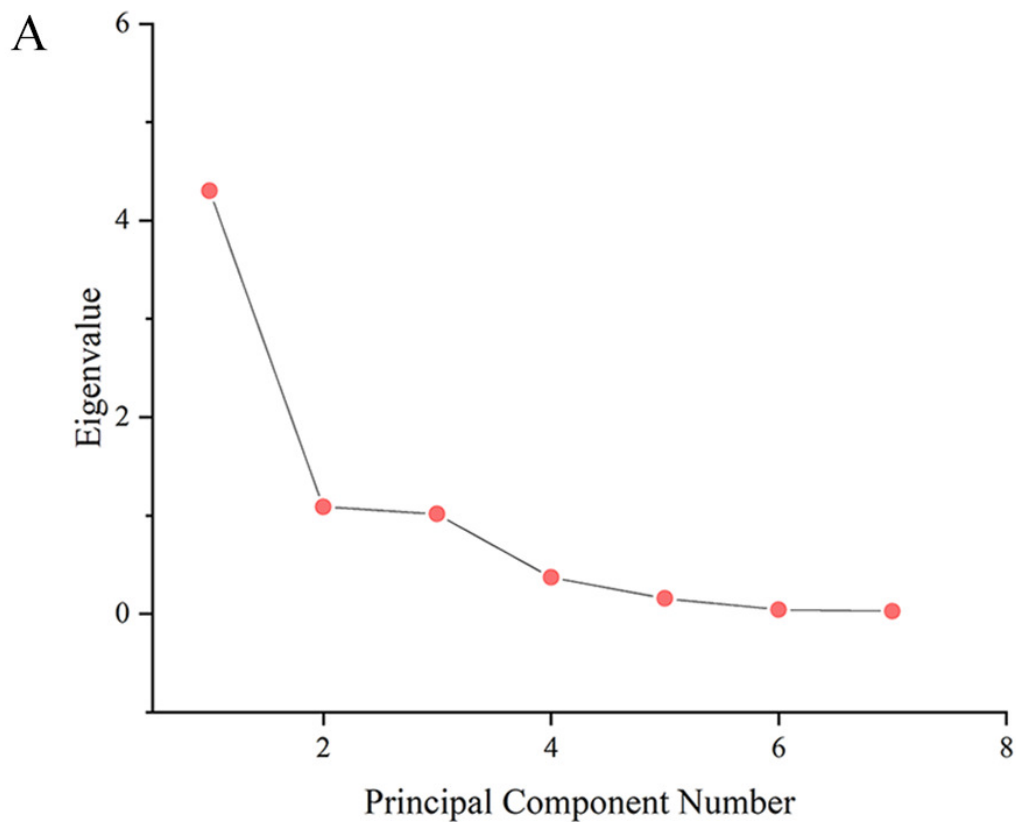
# Figure 4

Effect of MDP on the morphology of RAW264.7 cells (A) and the effect of MDP on RAW264.7 cell viability (B). The values are presented as the mean ± SD, n = 3. **$P <$ 0.01 *vs* control group .
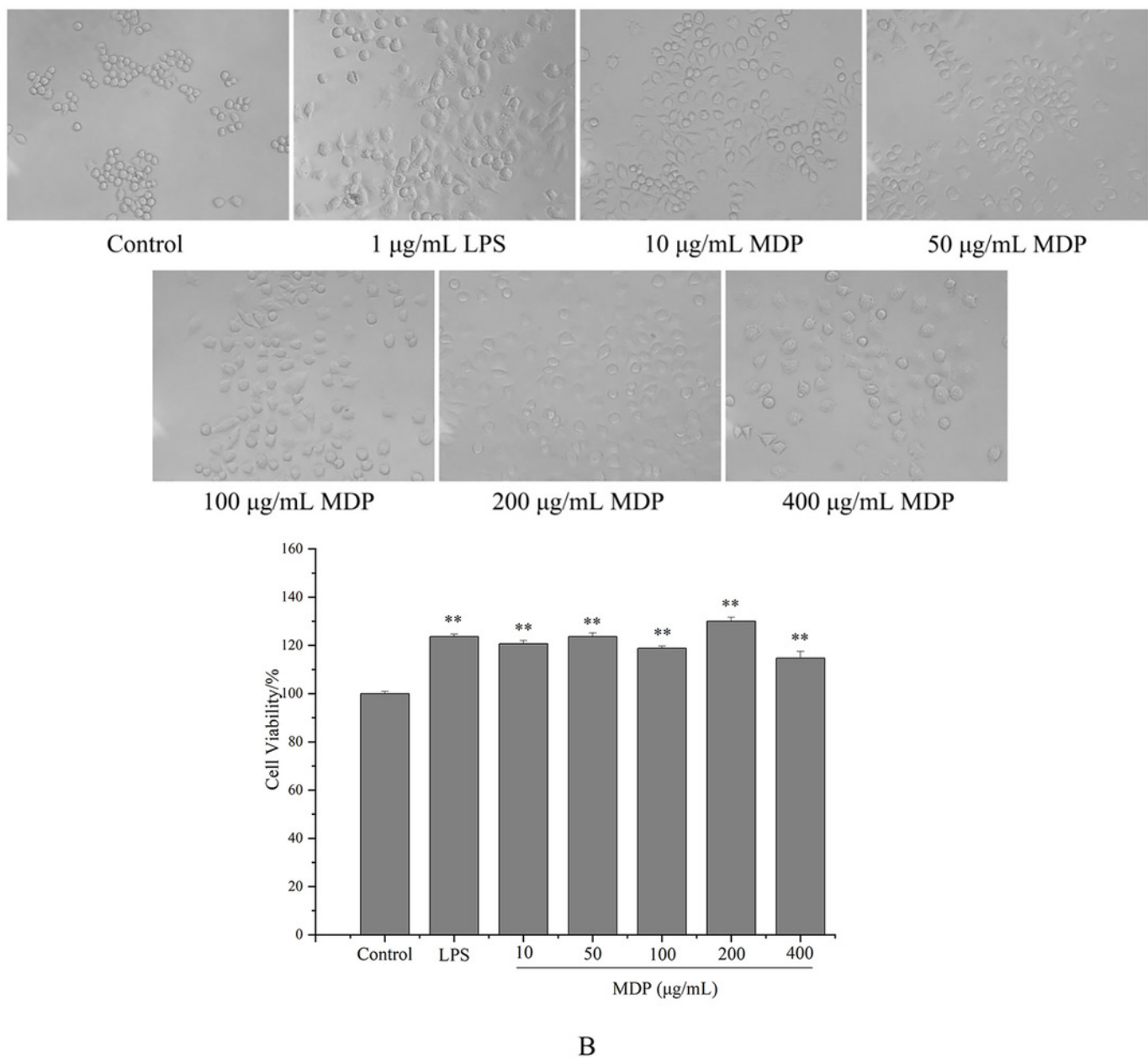
# Figure 5

Effects of MDP on the secretion of NO and cytokines with or without inhibitors.

(A) NO; (B) TNF-α; (C) IL-6. Without inhibitors, the secretion of NO and cytokines by macrophages was induced by MDP, however, this impact was hindered when the RAW264.7 cells had been pre-treated with inhibitors. The values are presented as the mean ± SD, n = 3. *$P<0.05$, **$P<0.01$, compared with Control group. #$P<0.05$, ##$P<0.01$, compared with the no inhibitor group.
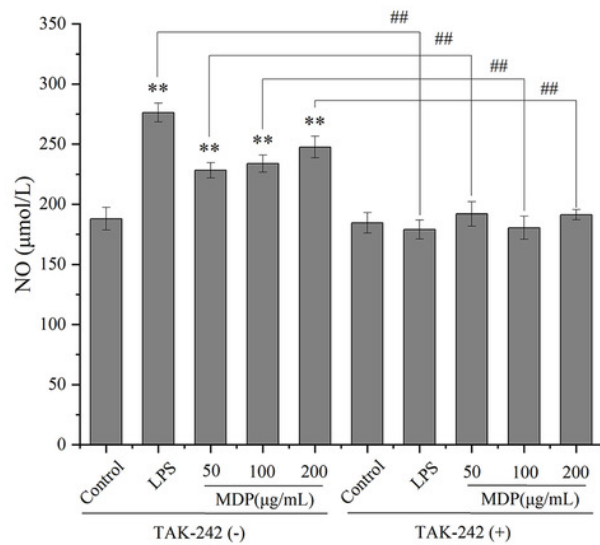
A
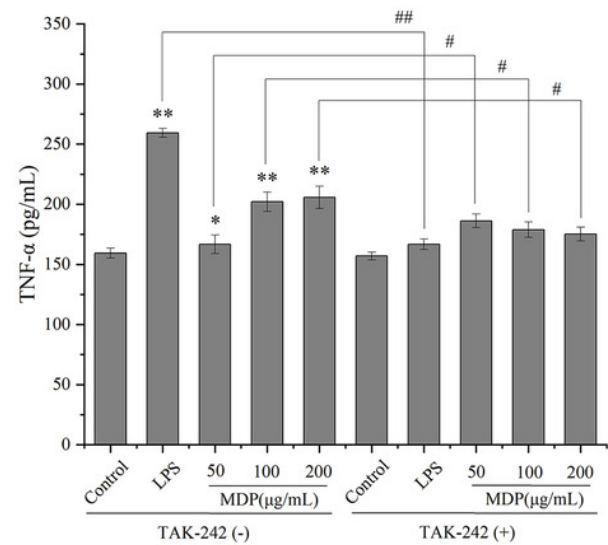
B
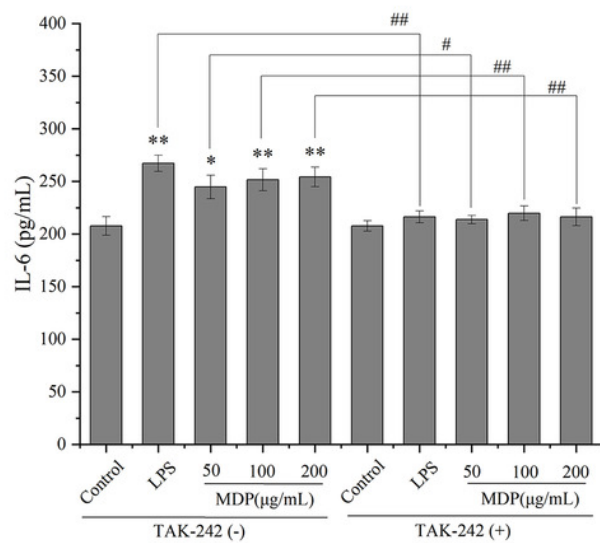
C

# Figure 6

The influence of MDP on the stimulation of TLR4-MAPK/NFκB signaling pathways in RAW 264.7 cells.

(A) TLR4, (B) MyD88, (C) p-NFκB/ NFκB, (D) p-ERK/ ERK, (E) p-JNK/JNK, (F) p-P38/ P38. The values are presented as the mean ± SD, n = 3. $*P<0.05$, $**P<0.01$, compared with Control group.
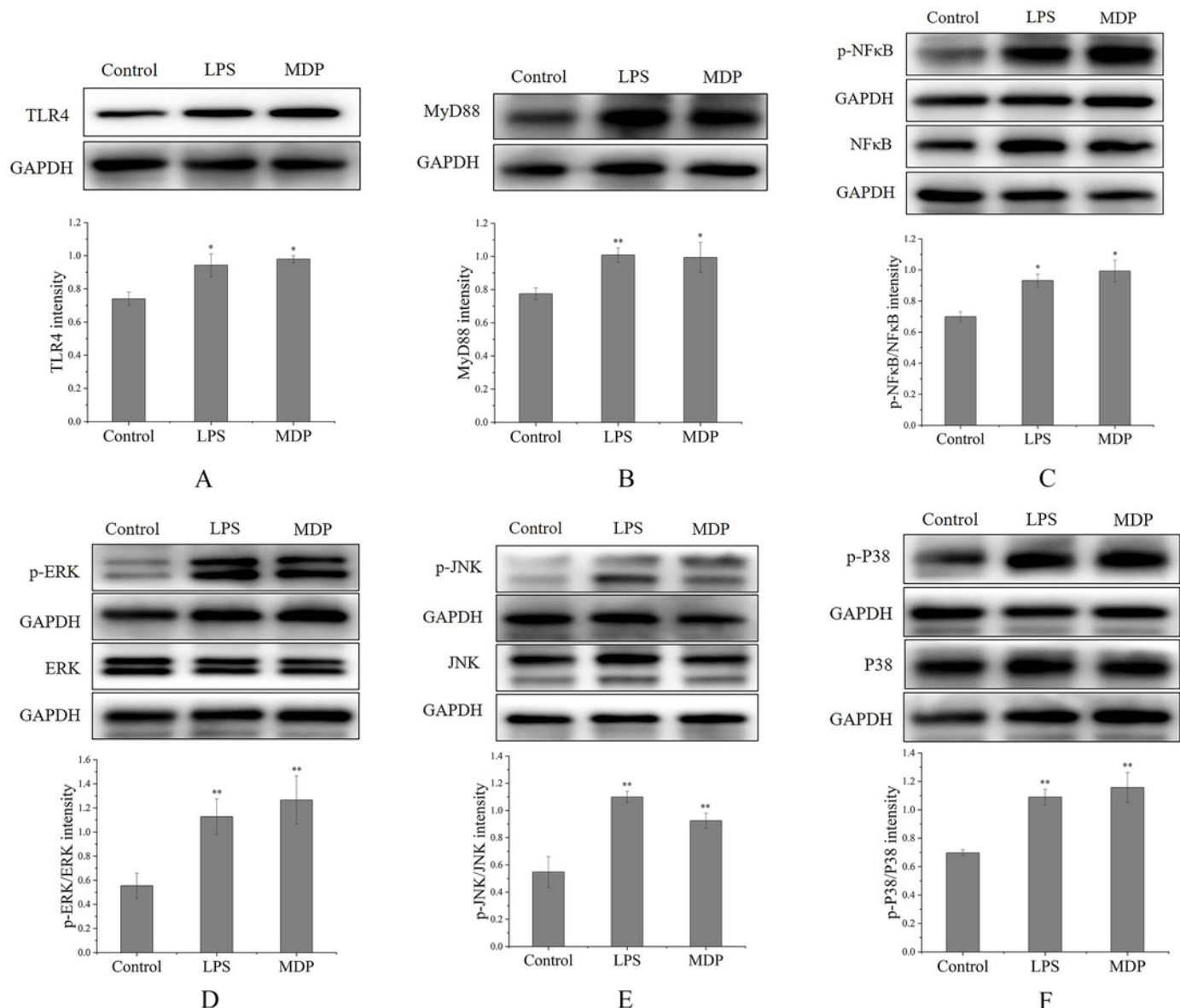
# Figure 7

Possible immunomodulatory signaling mechanism of MDP in RAW264.7 macrophages.